DOI: 10.1002/ejic.200900418

Preparation of Hollow Carbon and Silicon Carbide Fibers with Different Cross-Sections by using Electrospun Fibers as Templates

Yongliang Cheng,[a,b] Jiangfeng Zhang,[a,b] Yanfei Zhang,[a,b] Xiaolong Chen,[a,b] Ying Wang,[a] Hongmei Ma,[a] and Xueqiang Cao*[a]

Keywords: Nanostructures / Silicon / Carbides / Electrospinning / Template synthesis

Hollow carbon nanofibers with circular and rectangular opening were prepared by using electrospun silica fibers as templates. Silica fibers were synthesized by electrospinning, and they were coated with a carbon layer formed by thermal decomposition and carbonization of polystyrene under a nitrogen atmosphere. Hollow carbon nanofibers with circular and rectangular openings were then obtained after the silica core was etched by hydrofluoric acid. The carbon nanofibers with different morphologies also could be used as templates to fabricate silicon carbide fibers. The silicon carbide fibers with circular and rectangular openings could be obtained by using hollow carbon nanofibers and carbon belts as templates, respectively. The hollow carbon nanofibers and silicon carbide fibers were characterized by scanning electron microscopy, transmission electron microscopy, X-ray diffraction, and Raman spectroscopy, and the formation mechanism was also discussed

(© Wiley-VCH Verlag GmbH & Co. KGaA, 69451 Weinheim, Germany, 2009)

Introduction

Since the discovery of carbon nanotubes,[1] 1D carbon materials such as nanotubes and nanofibers have been drawing attention because of their important applications in sensors,[2] catalysis,[3] hydrogen storage,[4] and electron field emitters.[5] Various methods have been developed to prepare carbon nanotubes, including laser ablation,[6] chemical vapor deposition (CVD),[7] and catalytic decomposition of hydrocarbons.[8] Among these strategies, the template method has been widely applied, and anodic aluminum oxide (AAO) film and mesoporous silica are usually used as the templates. The morphology of carbon nanotubes is dependent on the carbon source[9] and preparation procedure.[10]

Silicon carbide is one of the most important semiconductor materials, as it possesses some excellent properties, including high thermal and chemical stability, high hardness and strength, which make it have potential applications in nanoscale electronics,[11] optics,[12] and field-emission devices.[13] Therefore, many methods, including carbothermal reduction,[14] CVD,[15] laser ablation,[16] and hydrothermal methods[17] have been developed to fabricate SiC nanomaterials. Unfortunately, the precursor gases ($SiCl_4$, CH_3SiCl_3) are toxic, corrosive, flammable, and explosive.[18] SiC synthesized by a carbon nanotube confined reaction usually are nanorods,[19] and the high cost of carbon nanotubes also restricts their application.

Recently, electrospinning has been extensively explored as an advantaged and facile method to create fibers with diameters ranging from tens of nanometers to several micrometers (Figure 1). Nanotubes or hollow nanofibers could be obtained by the decomposition of different shell materials on the electrospun fiber surface, which are called tubes by fiber template (TUFT). Caruso et al.[20] and Kim et al.[21] synthesized TiO_2 tubes by sol–gel coating and atomic layer deposition, respectively. Hou and co-workers described the preparation of poly(*p*-xylylene) nanotubes by chemical vapor deposition with electrospun fibers as templates.[22] Dong et al.[23] fabricated carbon nanofibers using polypyrrole as the carbon source and poly(methyl methacrylate) as templates through in situ polymerization. The group of Xia[24] fabricated carbon nanotubes by vapor deposition polymerization with electrospun poly(styrene sulfonate) sodium as core templates. In addition, metal nanotubes have also been prepared by electroless plating by using electrospun nanofibers as templates.[25]

Polystyrene (PS), a transparent, colorless, and brilliant material, is one of the most useful plastics. As a result of its thermally degradable peculiarity, PS is usually not used as a carbon source for the synthesis of carbon materials. Recently, it was reported that styrene and PS could be used as carbon sources to synthesize carbon materials with dif-

[a] State Key Laboratory of Rare Earth Resource Utilization, Changchun Institute of Applied Chemistry, Chinese Academy of Science,
Changchun 130022, Jilin, P. R. China
Fax: +86-461-85262285
E-mail: xcao@ciac.jl.cn
[b] Graduate School of the Chinese Academy of Sciences, Beijing 100049, P. R. China

Supporting information for this article is available on the WWW under http://dx.doi.org/10.1002/ejic.200900418.

 WILEY InterScience DISCOVER SOMETHING GREAT © 2009 Wiley-VCH Verlag GmbH & Co. KGaA, Weinheim

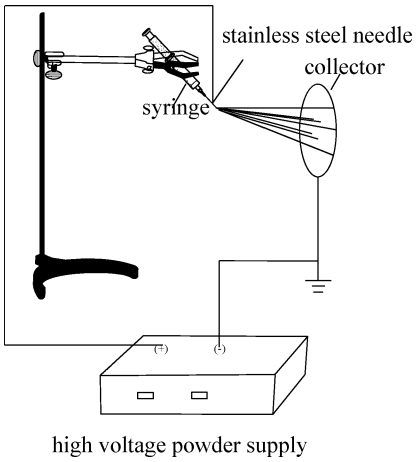

Figure 1. Schematic diagram of the electrospinning setup.

ferent morphologies. For example, Xia et al.[26] reported the synthesis of ordered mesoporous carbon with a graphitic pore wall by using styrene as the carbon source. Lei and coworkers reported the fabrication of ordered macroporous materials by using PS as a carbon source.[27]

In this paper, we employ economical polymer materials as a carbon source to synthesize hollow carbon nanofibers by using electrospun silica fibers as templates. Carbon fibers with circular and rectangular openings could be synthesized by the selection of different silica fiber templates. To the best of our knowledge, belt-like carbon fibers with a rectangular opening have not been reported. Furthermore, we synthesized SiC hollow nanofibers by using hollow carbon nanofibers as templates.

Results and Discussion

Structure of Hollow Carbon Nanofibers

XRD was applied to investigate the crystal structure of the carbon nanofibers. In the XRD pattern of the carbon nanofibers (Figure 2), the most intensive peak near 2θ = 22° should be indexed as the (002) reflection of the graphite lattice. This indicates that the synthesized carbon nanofibers are partially graphitized. As a result of the insufficiently ordered structures of carbon materials synthesized at low temperature, the (110) and (001) reflections are invisible by XRD.

The morphology, surface structure, and dimension of silica and carbon nanofibers were characterized by SEM. Figure 3a shows the representative images of silica nanofibers obtained by calcining the composite fibers at 700 °C. Even though PVP in the fibers was removed by thermal decomposition, the continuous 1D fiber structure is still retained, and the fiber has a very smooth surface.

After the carbonization of PS/silica fibers and etching of the silica template, hollow carbon nanofibers could be obtained, as shown in Figure 3b–d with different magnifications. These fibers are randomly oriented in the form of a nonwoven mat. The length of the carbon fibers ranges from several to tens of micrometers. The diameters of the hollow carbon nanofibers are in the range of 80 to 450 nm, and the average diameter is about 270 nm. The hollow structure indicates that removal of the silica core by etching does not result in the collapse of the fibers.

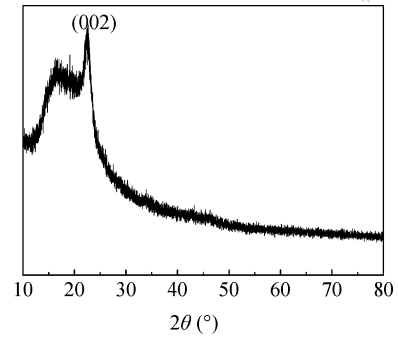

Figure 2. XRD pattern of hollow carbon nanofibers.

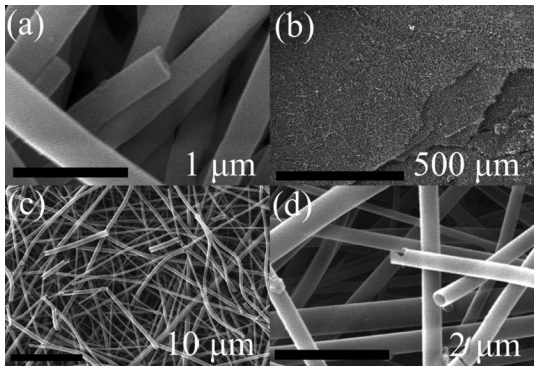

Figure 3. SEM images of silica fiber templates (a) and SEM images of hollow carbon nanofibers at different magnifications (b–d).

The morphologies and microstructures of the carbon nanofibers were further characterized by TEM and SAED (Figure 4). From Figure 4a we can observe that the carbon nanofibers have an apparent hollow structure. The wall thickness ranges from 10 to 20 nm. The ring-like SAED pattern indicates that the carbon nanofibers are partially graphitized. The diffraction ring can be indexed to reflection (002).

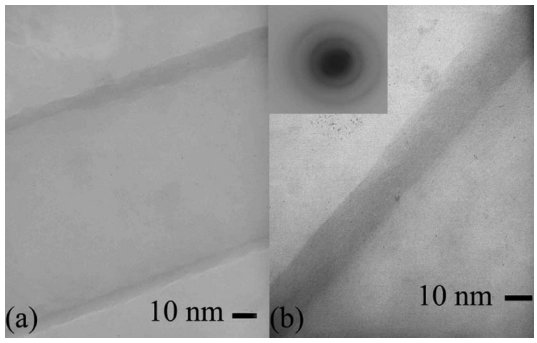

Figure 4. TEM images of hollow carbon nanofibers. The inset in (b) corresponds to the SAED of the hollow carbon nanofibers.

 © 2009 Wiley-VCH Verlag GmbH & Co. KGaA, Weinheim

Figure 5 shows the Raman spectrum of the hollow carbon nanofibers. The spectrum is very similar to those reported in the literature for other carbon nanotubes.[28] The strong and relatively narrow band around 1584 cm^{-1} corresponds to the E_{2g} vibration mode of the graphite layer with sp^2 bonding (G-band), and the broad band at 1344 cm^{-1} corresponds to the A_{1g} mode for the disordered graphite structures caused by sp^3 bonding (D-band). As a result of the different preparation procedures of the carbon materials, the G- and D-bands have slight variations both in their Raman shifts and their relative intensities, depending on the crystal planar domain size of graphite. The value can be obtained according to the following expression:

$$I_{max}(D)/I_{max}(G) = C(\lambda)/L$$

where L is the size of the graphite nanoflakes, C = 4.4 nm, and λ = 514.5 nm. On the basis of these parameters, L is calculated to be 5.2 nm.

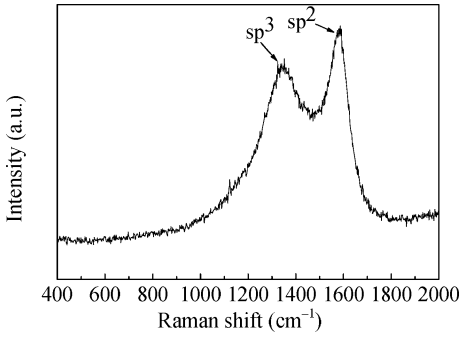

Figure 5. Raman shift of hollow carbon nanofibers.

Figure 6 shows the TGA curve of the SiO_2/carbon composite synthesized at 800 and 1000 °C. The yield and the thermal stability of the carbon nanofibers could be obtained from TGA measurements of the SiO_2/carbon composite fibers. Because the oxidation temperature of carbon materials is strongly influenced by the wall defects, the oxidation reaction first occurs at the graphite layer edge defects and on the disordered graphite layer. In general, oxidation of ideal graphite begins above 600 °C, which has a higher thermal stability than amorphous carbon and less order than graphite.[29] From the TGA curve, we could observe that the yields of the hollow carbon nanofibers are 14% at 800 °C and 22% at 1000 °C. The phenomenon of different yields at different temperatures could be attributed to the fact that some gas decomposed from PS was not completely carbonized at low temperature and the residual gas was carbonized at higher temperature. It is clear that the hollow carbon nanofibers synthesized at 1000 °C have higher thermal stability than the fibers synthesized at 800 °C, which could be attributed to the fact that the graphitization was improved at higher synthesis temperature.

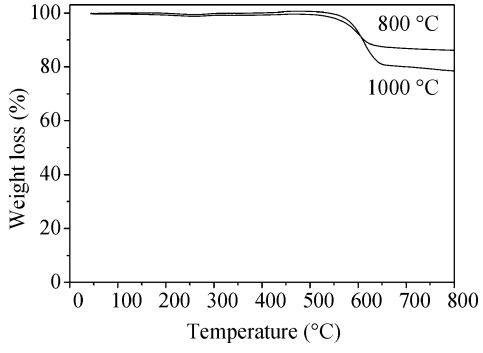

Figure 6. TGA of the SiO_2/carbon composite synthesized at 800 and 1000 °C.

Structure of Hollow SiC Nanofibers

As shown in the XRD pattern (Figure 7), the SiC nanofibers were successfully synthesized by using hollow carbon nanofibers as templates. The main peaks in the XRD pattern are assigned to the (111), (200), (220), and (311) reflections of cubic β-SiC, in agreement with the standard JCPDS card (No. 65–0360). An additional diffraction peak at 2θ = 33.64° is characteristic of stacking faults on the [111] plane in the SiC nanofibers, which has also been observed in the literature.[30]

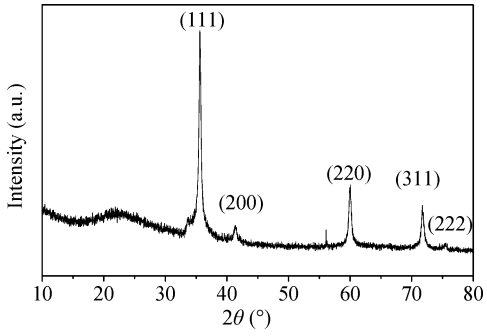

Figure 7. XRD pattern of SiC hollow nanofibers.

Figure 8 shows the representative SEM and TEM images of SiC nanofibers obtained by the reaction at 1300 °C. As shown in Figure 8a, the 1D fiber structure is still retained, and the surface of SiC becomes rougher than that of the hollow carbon nanofibers as a result of the transformation of carbon into SiC. The diameter of the SiC fibers is about 385 nm. From the high magnification SEM images (Figure 8b), it could be clearly seen that these nanofibers have an apparent open-tubular structure.

The morphology and microstructure of the SiC nanofibers were further characterized by TEM and SAED (Figure 8c,d); the SiC nanofibers have an open-tubular structure and a wall thickness of about 45 nm. SAED shows diffused rings, suggesting that the sample is polycrystalline.

In the case of transformation of carbon into SiC, the volume of SiC has swelled to some extent. The swell ratio could be concluded by the following expression:

$$V_{SiC} = V_C \frac{\rho_C}{\rho_{SiC}}\left(1 + \frac{M_{Si}}{M_C}\right)$$

where V_C, ρ_C, and M_C are the volume, density, and molecular weight of the hollow carbon nanofibers, and V_{SiC}, ρ_{SiC},

 © 2009 Wiley-VCH Verlag GmbH & Co. KGaA, Weinheim

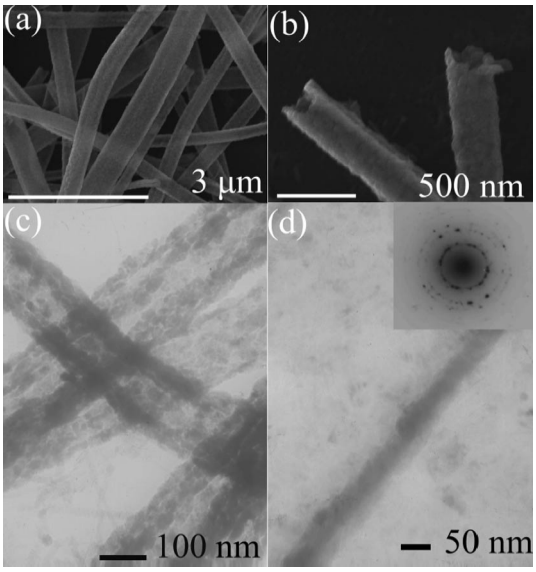

Figure 8. The SEM images (a,b) and TEM images (c,d) of SiC nanofibers. The inset in (d) corresponds to the SAED of the SiC nanofibers.

and M_{SiC} are the volume, density, and molecular weight of the hollow SiC nanofibers.[31] The value of V_{SiC}/V_C is approximately 2.2, and the diameter swells about 40% in our case.

Further characterization of SiC was investigated with FTIR. Figure 9 displays the characteristic IR spectrum of the SiC nanostructure. There are two absorption bands at around 472 and 1090 cm^{-1}, which correspond to Si–O stretching vibrations of amorphous SiO_2. The intense band at 821 cm^{-1} is induced by the TO phonons of SiC, and the absorption bands centered at 1634 and 3423 cm^{-1} are attributed to water.

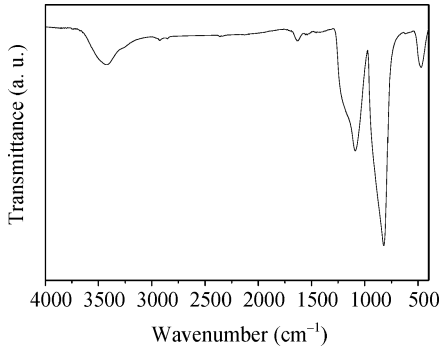

Figure 9. FTIR spectrum of hollow SiC nanofibers.

Figure 10 shows the nitrogen adsorption–desorption isotherm and pore-size distribution of the hollow carbon nanofibers and SiC nanofibers. The Brunauer–Emmett–Teller (BET) surface area of the hollow carbon nanofibers is 112.3 $m^2 g^{-1}$. The Barrett–Joyner–Halenda (BJH) method was used to calculate the pore-size distribution, and the result is shown in the Figure 10b. The carbon nanofibers have a wide pore-size distribution from 2 to 120 nm, which could be mainly attributed to the pore formed by a random stack of fibers. After transformation into SiC, the BET surface area of the SiC fibers is reduced to 29.4 $m^2 g^{-1}$, and the pore-size distribution as shown in Figure 10d is between 1.8 and 100 nm.

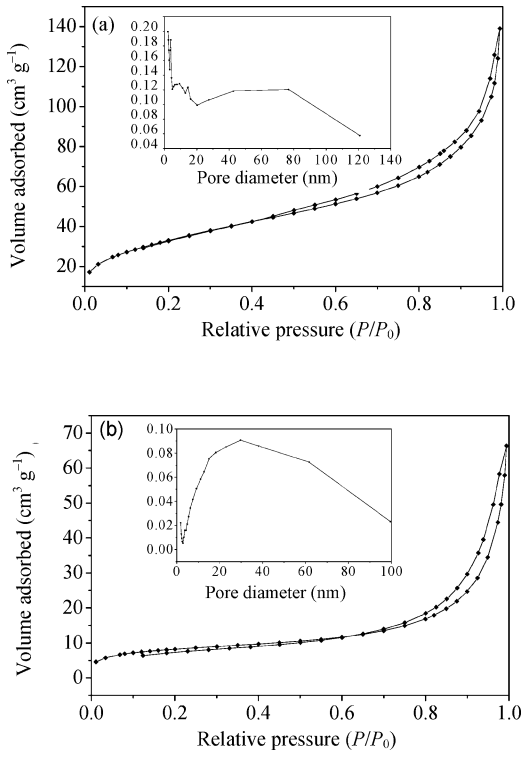

Figure 10. The nitrogen adsorption–desorption isotherm and pore-size distribution (insert) of hollow carbon nanofibers (a) and SiC fibers (b).

Electrospinning is a complicated process. Many factors have strong influences on the morphologies and microstructures of the electrospun fibers, such as polymer concentration, volatility of solvent, strength of electric field, feeding rate of the precursor, and ambient parameters including temperature and humidity. In our experiment, when the amount of TEOS (tetraethylorthosilicate) was increased to 3.0 mL and the other conditions were kept constant, the morphology of the silica fibers changed into a belt, as shown in Figure 11a,b. These belt-like silica have a width and thickness of about 1 μm and 250 nm, respectively, and lengths up to tens of micrometers. In order to investigate the influence of the amount of TEOS on the morphologies of the silica fibers, we also fabricated silica fibers with other amounts of TEOS. When the amount of TEOS was decreased to 0.5 mL, the silica fibers became network-like (Supporting Information, Figure S1a), and when the amount of TEOS was increased to 6.0 mL, the width of the silica belts increased to about 2 μm (Supporting Information, Figure S1b). In the process of electrospinning, TEOS would become a gel because of the rapid evaporation of the solvent. So, if the amount of TEOS was not enough, although composite fibers with a circular cross-section could be collected on the collector (Supporting Information, Figure S2a), TEOS could not form a complete gel

 © 2009 Wiley-VCH Verlag GmbH & Co. KGaA, Weinheim

layer on the surface of the electrospun composite fibers, and TEOS inside the composite fibers would connect to each other in the interface of composite fibers and become a network-like morphology in the process of heat treatment. By increasing the amount of TEOS to 1.5 mL, although the morphologies of the composite fibers obtained are fibers with a circular cross-section, a complete silica gel layer on the surface of the composite fibers could form in the process of electrospinning, which could prevent silica from connecting to each other during heat treatment, so silica fibers with a 1D morphology rather than a network-like morphology could be obtained after annealing at high temperature. If the amount of TEOS was further increased to 3.0 mL, the silica gel layer would become thicker and hinder the evaporation of solvent inside the composite fibers, so the inside of the composite is not completely dried and the silica gel layer does not have enough rigidity to keep the fiber morphology, so the composite fibers would collapse and composite belts could be formed (Supporting Information, Figure S2c). After annealing at high temperature, silica belts could form. By further increasing the amount of TEOS, the width of the silica belt would become large and the belt-like morphologies could not be changed Supporting Information, Figure S2d).

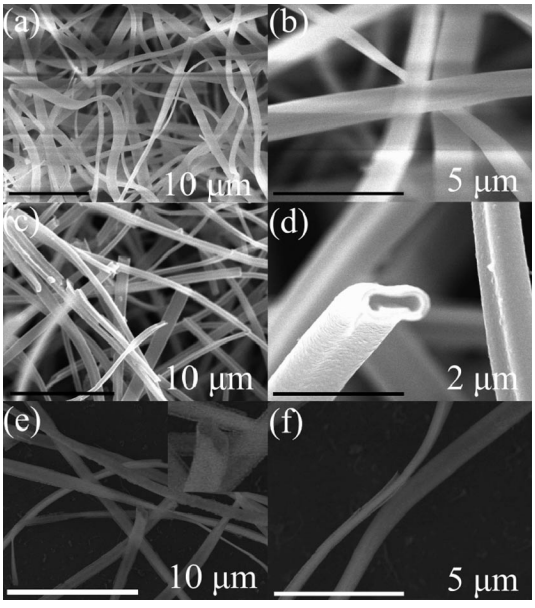

Figure 11. SEM images of silica belt templates (a,b), carbon belts (c,d), and SiC belts (e,f) at different magnifications.

Figure 11c,d are typical SEM images of the carbon fibers synthesized by using belt-like silica as template. The carbon fibers have belt-like morphologies; the widths and thicknesses of these carbon belts are about 1 μm and 250 nm, respectively, which are similar to those of SiO_2 belts. The high-magnification SEM image shows that the belt-like carbon fibers have a rectangular open-tubular structure, which indicates that etching of the silica templates does not result in the collapse of the fibers (Figure 11d). Although the group of Lee[32] reported the fabrication of quasi 2D carbon nanobelts by thermal decomposition of ethanol on nanoporous alumina templates, the formation of these nanobelts is attributed to the collapse of the nanotubes, because the carbon shell is too thin to have enough rigidity to keep their hollow tube-like morphologies. The carbon belts synthesized by this method have a rectangular open-tubular structure and did not collapse after removal of the SiO_2 templates, which should be attributed to the fact that the carbon shell has enough rigidity to retain their morphologies when enough PS is used as the carbon source. In the process to fabricate hollow carbon nanofibers with circular openings, we also found that carbon fibers with irregular openings (Supporting Information, Figure S3a–c) and some carbon belts (Supporting Information, Figure S3c), also could be found if the amount of silica nanofiber templates is increased to 0.10 g. This phenomenon should be attributed to the fact that the carbon produced form the decomposition of PS was not enough; the carbon shell does not have enough rigidity to retain their hollow structure after removal of the silica templates, so the carbon shell would collapse into belts and fibers with irregular openings. Because the amount of carbon decomposed from PS was not enough, some silica fibers were not completely covered by the carbon shell, and trough-like carbon could also be found (Supporting Information, Figure S3d). So, the key factor for formation of carbon belts with rectangular openings is the existence of enough carbon source to ensure that the carbon shells have enough rigidity to retain their hollow morphologies so that they do not collapse after removal of the silica templates. Carbon belts with this morphology have never been reported in the literature.

The SEM images of SiC fabricated by using belt-like carbon fibers as a template are shown in Figure 11e,f. The SiC fibers also have belt-like morphologies even in the high-temperature reaction. The inset image of Figure 11e shows that the cross-sections of the SiC belts are also rectangular.

Formation Mechanism of Hollow Carbon and SiC Fibers

The formation process of hollow carbon and SiC fibers is described in Figure 12. The silica nanofibers are dispersed into PS solution, and after the solvent is evaporated, the silica nanofibers and PS are interconnected. During the heat treatment, PS decomposes into its monomer, dimer, trimer, and so on, and some part is carbonized on the silica fiber surface. If silica fibers are not used, the carbon would fly away into the flowing nitrogen. The silica nanofiber acts as the template during the whole process of PS decomposition and carbonization of the decomposed species.[33] When the silica core is removed by HF, hollow carbon nanofibers are formed. When the SiO_2 belts instead of the SiO_2 fibers were used as templates, carbon microbelts with rectangular openings could be obtained. The resulting carbon fibers and belts could well replicate their template shapes, which indicted shape memory was retained during the synthesis process from SiO_2 templates to carbon fibers and belts.

When the carbon fibers are used as templates to fabricate SiC fibers, the formation of SiC involved in a solid–gas re-

 © 2009 Wiley-VCH Verlag GmbH & Co. KGaA, Weinheim

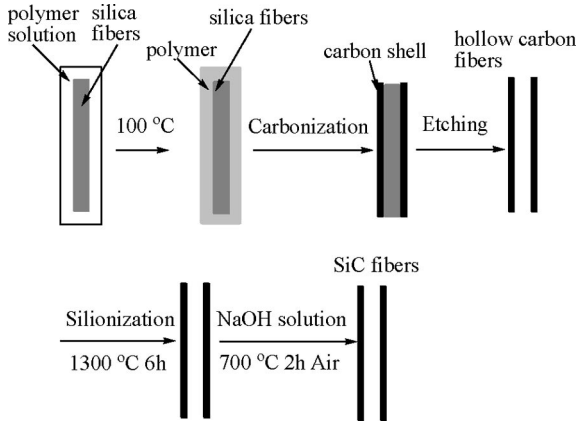

Figure 12. Formation procedure of the hollow carbon and SiC nanofibers.

action between carbon and Si vapor generated from Si solid powder at high temperature. The main reaction involved in this synthesis process could be illustrated by the reactions outlined in Equations (1) and (2).

$$Si(s) \rightarrow Si(g) \quad (1)$$

$$Si(g) + C(s) \rightarrow SiC(s) \quad (2)$$

In the synthesis process, the carbon fibers not only acts as the carbon source but also as the template during the conversion from carbon into SiC fibers, so the resulting SiC could well keep the original morphologies of the carbon fibers. The SiC hollow fibers with circular and rectangular openings could be synthesized by choosing hollow carbon nanofibers and carbon belts, respectively.

Conclusions

In summary, hollow carbon and SiC fibers were fabricated by using electrospun SiO_2 and carbon fibers as templates, respectively. The morphologies of the carbon fibers could be tuned from fibers to belts and the openings changed from circular to rectangular when SiO_2 belts instead of SiO_2 fibers were used as templates The inner diameters and morphologies of the carbon nanofibers were similar to those of SiO_2 templates. The hollow SiC fibers and belts could also be fabricated by using carbon fibers as templates. The morphologies of the SiC fibers depend on the morphologies of the carbon fibers.

Experimental Section

General Methods: Structure analysis with X-ray diffraction (XRD) was performed with a Rigaku D/MAX-2500 diffractometer. The morphology of the carbon nanofibers was analyzed by scanning electron microscope (SEM, XL 30 ESEM FEG, Micro FEI Philips) and transmission electron microscope (TEM). SAED (selected area electron diffraction) were recorded with a JEOL-JEM-2010 operating at 200 kV (JEOL, Japan). Raman spectroscopy was recorded with a JY T4–6000 Raman with an excitation wavelength of 514.5 nm. Thermal gravimetric analysis was performed with a thermoanalyzer (Pyris Diamond TG/DTA) in air with a heating rate of 10 °C min^{-1}. Specific surface areas of the fibers were measured by N_2 adsorption–desorption isotherm at 77 K with a Micromeritics ASAP2020 instrument. Fourier-transformed infrared (FTIR) spectra were recorded with a Bruker Vertex 70 FTIR spectrometer in the range 400–4000 cm.

General Procedure for the Preparation of the Silica Nanofibers: A solution composed of deionized water (1.0 mL), hydrochloric acid (0.23 mL, 1.2 M), tetraethylorthosilicate (TEOS, 1.5 mL) and polyvinylpyrrolidone (PVP, 4.00 g) was magnetically stirred at room temperature for 3.3 h, resulting in the formation of a transparent solution for electrospinning. A typical electrospinning setup consists of three major components: high-voltage power supply, a plastic syringe with a stainless steel needle, which was used as the spinneret, and a grounded collector plate (Figure 1). In a typical electrospinning process, the electrospinning precursor solution is ejected from the stainless steel needle with a voltage of 30 kV. The distance between the capillary and collector was 15 cm. As a result of the evaporation of the solvent, the composite fibers in the form of nonwoven mats could be collected on the collector. The as-prepared precursor fibers were calcined at 700 °C for 4 h with a heating rate of 1 °C min^{-1}.

PS (1.00 g) was dissolved in dimethylformamide to form a homogeneous solution. Subsequently, silica nanofibers (0.040 g) were dispersed into the PS solution. The solution was simply evaporated in a dish, and the as-obtained PS-silica composite nanofiber was treated at 800 °C for 2 h with a heating rate of 5 °C min^{-1} under a nitrogen atmosphere. After the carbonization, the silica nanofibers were removed with hydrofluoric acid for 12 h at room temperature. The hollow carbon nanofibers were washed with deionized water and dried at 100 °C overnight.

The carbon fiber templates used to fabricate SiC fibers were synthesized at 1000 °C and other conditions were kept constant. The hollow carbon nanofibers were first mixed with an excess amount of silicon powder, and then, the mixture was treated at 1300 °C for 6 h with a heating rate of 5 °C min^{-1} under an argon atmosphere. The resulted powder was treated with 5 M NaOH solution and then washed with distilled water several times and dried at 100 °C. Finally, the powder was calcined at 700 °C for 2 h in air.

Supporting Information (see footnote on the first page of this article): SEM images of SiO_2 fibers fabricated with different amounts of TEOS; SEM images of composite fibers with different amounts of TEOS; SEM images of carbon nanofibers with different openings.

Acknowledgments

This work was financially supported by the National Natural Science Foundation of China (NSFC) (50825204).

[1] S. Iijima, *Nature* **1991**, *354*, 56–58.
[2] J. Kong, N. R. Franklin, C. W. Zhou, M. G. Chaplin, S. Peng, K. Cho, H. Dai, *Science* **2000**, *287*, 622–625.
[3] R. Ryoo, S. H. Joo, M. Kruk, M. Jaroniec, *Adv. Mater.* **2001**, *13*, 677–681.
[4] G. Mpourmpakis, E. Tylianakis, G. E. Froudakis, *Nano Lett.* **2007**, *7*, 1893–1897.
[5] Y. S. Chen, J. H. Huang, J. L. Hu, C. C. Yang, W. P. Kang, *Carbon* **2007**, *45*, 3007–3014.
[6] T. Azami, D. Kasuya, T. Yoshitake, Y. Kubo, M. Yudasaka, T. Ichihashi, S. Iijima, *Carbon* **2007**, *45*, 1364–1369.

 © 2009 Wiley-VCH Verlag GmbH & Co. KGaA, Weinheim

[7] S. Bhaviripudi, E. Mile, S. A. Steiner, A. T. Zare, M. S. Dresselhaus, A. M. Belcher, J. Kong, *J. Am. Chem. Soc.* **2007**, *129*, 1516–1517.
[8] P. B. Amama, S. Lim, D. Ciuparu, Y. H. Yang, L. Pfefferle, G. L. Haller, *J. Phys. Chem. B* **2005**, *109*, 26452656.
[9] a) A. T. Rodriguez, M. Chen, Z. Chen, C. J. Brinker, H. Y. Fan, *J. Am. Chem. Soc.* **2006**, *128*, 9276–9277; b) J. T. Chen, K. Shin, J. M. Leiston-Belanger, M. F. Zhang, T. P. Russell, *Adv. Funct. Mater.* **2006**, *16*, 1476–1480; c) C. H. Huang, Y. H. Chang, H. W. Wang, S. Cheng, C. Y. Lee, H. F. Chin, *J. Phys. Chem. B* **2006**, *110*, 11818–11822.
[10] a) Z. H. Wen, Q. Wang, J. H. Li, *Adv. Funct. Mater.* **2008**, *18*, 959–964; b) J. C. Bao, K. Wang, Z. Xu, H. Zhang, Z. H. Lu, *Chem. Commun.* **2003**, 208–209.
[11] H. K. Seong, H. J. Choi, S. K. Lee, J. I. Lee, D. J. Choi, *Appl. Phys. Lett.* **2004**, *7*, 1256–1259.
[12] Z. J. Li, J. L. Zhang, A. L. Meng, J. Z. Guo, *J. Phys. Chem. B* **2006**, *110*, 22382–22386.
[13] Y. J. Yang, G. W. Meng, X. Y. Liu, L. D. Zhang, D. Z. Hu, C. Y. He, Y. M. Hu, *J. Phys. Chem. C* **2008**, *112*, 20126–20130.
[14] Z. X. Yang, Y. D. Xia, R. Mokaya, *Chem. Mater.* **2004**, *16*, 3877–3884.
[15] Y. Kamlag, A. Goossens, I. Colebeck, J. Schoonman, *Chem. Vap. Deposition* **2003**, *9*, 125–129.
[16] T. Tomita, K. Kinoshita, S. Matsuo, S. Hashimoto, *Appl. Phys. Lett.* **2007**, *90*, 153115–153117.
[17] L. Z. Pei, Y. H. Tang, Y. W. Chen, C. Guo, X. X. Li, Y. Yuan, Y. Zhang, *J. Appl. Phys.* **2006**, *99*, 114306–114311.
[18] R. L. Choy, *Prog. Mater. Sci.* **2003**, *48*, 57–170.
[19] R. B. Wu, G. Y. Yang, Y. Pan, J. J. Chen, *J. Mater. Sci.* **2007**, *42*, 3800–3804.
[20] R. A. Caruso, J. H. Schattka, A. Greiner, *Adv. Mater.* **2001**, *13*, 1577–1579.
[21] G. K. Kim, S. M. Lee, G. H. Michler, H. Roggendorf, U. Gosele, M. Knez, *Chem. Mater.* **2008**, *20*, 3085–3091.
[22] H. Q. Hou, Z. Jun, A. Reuning, A. Schaper, J. H. Wendorff, *Macromolecules* **2002**, *35*, 2429–2431.
[23] H. Dong, S. Prasad, V. Nyame, W. E. Jones Jr, *Chem. Mater.* **2004**, *16*, 371–373.
[24] J. T. McCann, B. Lim, R. Ostermann, M. Rycenga, M. Marquez, Y. N. Xia, *Nano Lett.* **2007**, *7*, 2470–2474.
[25] F. Ochanda, W. E. Jones Jr, *Langmuir* **2005**, *21*, 10791–10796.
[26] Y. D. Xia, R. Mokaya, *Adv. Mater.* **2004**, *16*, 1553–1558.
[27] Z. B. Lei, Y. Xiao, L. Q. Dang, W. S. You, G. S. Hu, J. Zhang, *Chem. Mater.* **2007**, *19*, 477–484.
[28] N. A. Katcho, E. Urones-Garrote, D. Avila-Brande, A. Gómez-Herrero, S. Urbonaite, S. Csillag, E. Lomba, F. Agulló-Rueda, A. R. Landa-Cánovas, L. C. Otero-Díaz, *Chem. Mater.* **2007**, *19*, 2304–2309.
[29] a) Q. W. Li, H. Y. B. Ye, J. Zhang, Z. F. Liu, *J. Phys. Chem. B* **2006**, *43*, 11085–11088; b) A. Bakandritsos, A. Smopoudos, D. Petridis, *Chem. Mater.* **2005**, *17*, 3468–3474.
[30] Y. Shin, C. Wang, G. J. Exarhos, *Adv. Mater.* **2005**, *17*, 73–77.
[31] T. Taguchi, N. Igawa, H. Yamamoto, S. I. Shamoto, S. Iitskawa, *Phys. E* **2005**, *28*, 431–438.
[32] C. T. Lin, T. H. Chen, T. S. Chin, C. Y. Lee, H. T. Chiu, *Carbon* **2008**, *46*, 741–746.
[33] S. W. Woo, K. Dokko, K. Sasajima, T. Takei, K. Kanamura, *Chem. Commun.* **2006**, *39*, 4099–4101.

Received: May 8, 2009
Published Online: August 26, 2009

 © 2009 Wiley-VCH Verlag GmbH & Co. KGaA, Weinheim